A Simplified Deformation Estimation Method for Anchor Piles of Sheet Pile Quay Walls under Kinematic Forces during Earthquakes

Kenichiro Miyashita
Pacific Consultants Co, Ltd, Japan
kenichirou.miyashita@os.pacific.co.jp
(corresponding author)

Takashi Nagao
Kobe University, Japan
nagao@people.kobe-u.ac.jp

ABSTRACT

In the seismic design of quay walls, it is necessary to evaluate the deformation of the walls during earthquakes as well as the safety of structural members. However, conventional seismic design methods for sheet pile quay walls cannot accurately determine the degree of deformation. One reason for this is that conventional methods do not consider kinematic forces acting on an anchor pile due to the deformation of the ground. This study proposes a simplified estimation method for anchor pile deformation under the influence of kinematic forces. The results of two-dimensional finite element analysis reveal that anchor pile deformation involves rotational and translational components caused by the kinematic forces, which the conventional methods do not consider. The deformation of the anchor pile caused by kinematic forces was 30%–40% of the total deformation at the pile head. It was clarified that unlike horizontally stratified ground, shear stress is generated in the ground before an earthquake resulting in the kinematic force acting on the anchor pile during the earthquake. Furthermore, a simplified method for estimating the deformation of the anchor pile under kinematic forces that uses one-dimensional seismic response analysis considering the predicted shear stress based on a theoretical equation is proposed. It was demonstrated that the proposed method accurately reproduces the anchor pile deformation.

I. INTRODUCTION

In the seismic design of structures, the seismic safety of structural members is the main focus of the assessment [1, 2]. Quay walls are a major part of port facilities, and are constructed on soft ground in coastal areas. In the event of an earthquake, seaward deformation of the quay walls can occur, which may interfere with the use of berths, even if the structural members are safe [3–6]. Therefore, in seismic design of quay walls, it is necessary to evaluate the degree of deformation of the quay wall with high accuracy. A sheet pile quay wall is a structure that is often constructed in quite soft ground. In areas where significant ground motions can occur, an anchor pile is often driven into the ground at a position away from the sheet pile to resist seismic forces. Conventional seismic design of anchor piles generally only considers tie rod tension and subgrade reaction as loads acting on the anchor piles [1]. Although this conventional method has been effective for designing safe cross-sections of piles to resist seismic forces, it predicts the deformation degree with low accuracy [7,

8]. Various studies have shown that two-dimensional (2D) Finite Element Analysis (FEA) can accurately reproduce the seismic deformation of quay walls [9–18]. However, 2D FEA is not a standard technique in design practice, due to its large computational burden. One reason for the low deformation calculation accuracy by the conventional method is because it does not consider the force generated by the deformation of the ground (kinematic force). Both inertial and kinematic forces act against a sheet pile quay wall during earthquakes [19–21]. However, the conventional method only considers inertial forces, such as hydrostatic and seismic earth pressure. Although several studies have been conducted on applying kinematic force to seismic design of piles [22–24], they focused on piles driven into horizontally stratified ground. To date, no studies have been conducted on piles under kinematic forces installed in uneven ground, such as that behind a sheet pile wall. This study proposes a simplified estimation method for the deformation of the anchor pile during earthquakes by kinematic forces. First, deformation of the anchor pile of a sheet pile quay wall was evaluated using 2D FEA. The bending

deformation of the anchor pile was calculated based on its curvature. By subtracting the bending deformation from the deformation of the anchor pile, its deformation due to kinematic forces was obtained. Because the ground in front of the anchor pile is not horizontally stratified, but irregular, shear stress is generated in this area before an earthquake and residual deformation occurs in the quay wall during the earthquake. We clarified that this is responsible for the kinematic force acting on the anchor pile during an earthquake. This paper proposes a simplified estimation method for the deformation of an anchor pile by kinematic forces. The method applies one-dimensional (1D) seismic response analysis considering an initial shear stress distribution in the ground predicted by a theoretical equation.

II. CONVENTIONAL SEISMIC DESIGN METHOD FOR ANCHOR PILES

The conventional method [1] assumes that an active failure region is generated behind the sheet pile and a passive failure region in front of the anchor pile. These regions are independent and do not affect each other (Figure 1). Here, each region is determined based on the seismic earth pressure by Mononobe-Okabe theory [25]. The anchor pile is located at the point where the active failure line is generated behind the sheet pile at the seabed level, which intersects the passive failure line generated in front of the anchor pile at $l_{m1}/3$ below the tie rod mounting height, where l_{m1} is the depth at which the bending moment of the anchor pile first becomes zero below the tie rod mounting height according to the Winkler foundation model. By installing the pile at this position, the conventional method assumes that the pile is embedded in horizontally stratified ground. Figure 2 shows the application method of the Winkler foundation model to the anchor pile. By applying the tie rod tension as a concentrated load and the subgrade reaction as a distributed load, the deformation magnitude and the cross-sectional force of the pile are calculated by solving the differential equation (1). Since the elongation of the tie rod is negligible, the deformation of the anchor pile is assumed to be equal to that of the quay wall.

$$EI \frac{d^4u}{dy^4} = -Bp \qquad (1)$$

where EI is the flexural rigidity of the pile, y is the depth, u is the lateral displacement of the pile at depth y, p is the subgrade reaction, and B is the pile width.
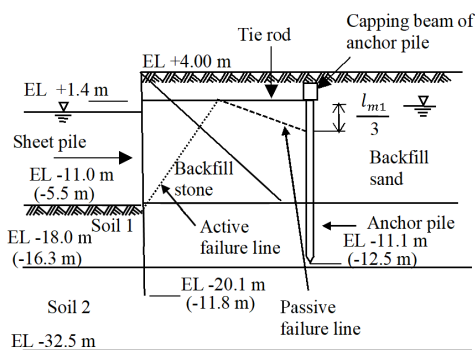

Fig. 1.   Profile of the studied sheet pile quay wall. Note: values in parentheses are the ones for water depth of 5.5m, EL: elevation.
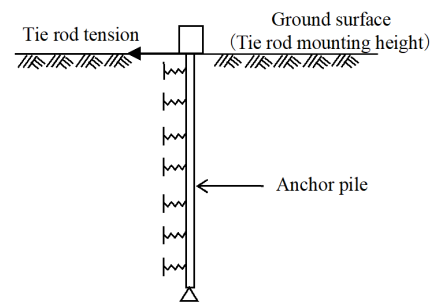

Fig. 2.   Forces applied to the pile.

The nonlinear load–displacement relationship of a pile is often modeled considering the nonlinear characteristics of the soil [26–28]. A nonlinear relationship between p and u is considered based on experimental test results as follows [1]:

$$p = k_c u^{0.5} \qquad (2)$$

$$p = k_s y u^{0.5} \qquad (3)$$

where k_s and k_c are the Subgrade Reaction Modulus (SRM) values for S-type and C-type ground, respectively. The ground is classified as S-type when the N-values obtained from the standard penetration test increase with increasing depth and as C-type when the N-value is independent of the depth. The current study used (2), assuming C-type of ground. The SRM is often considered to be dependent on the foundation width [29, 30], however, in the design of anchor piles, this dependence is ignored [1].

III. METHODS

Two sheet pile quay wall profiles designed according to [1] were used. As shown in Figure 1, the water depths were −5.5 and −11.0m, and the seismic coefficients were 0.10 and 0.15, respectively. The elevation of the ground surface was 4.0m. These values were set considering typical values used in design practice. Tables I and II list the ground conditions and dimensions of the structural members. The natural period of the ground was set to 0.8s for both ground conditions based on the values typically observed in the field. This study applied the FEA code FLIP [31], which is widely used for evaluating the seismic response of port facilities. Accurate reproduction of the seismic responses of various quay walls and grounds has been demonstrated using this code [32–34]. The code includes the multi-spring model for the ground [35] which considers the ground response under principal stress axis rotation. The nonlinear characteristics of the soil were modeled using the hyperbolic model [36] and (4) and (5). The hyperbolic model shows a substantial damping coefficient compared with the experimental result in the large shear strain range. Thus, the code modifies the hysteresis curve to reduce the area of the hysteresis loop compared to that given by the Masing rule [37] to prevent the damping coefficient from exceeding the maximum value, as shown in Table I [38]. The shear modulus of the soil was assumed to be dependent on the effective confining stress, as shown in (6).

$$\tau = \frac{G\gamma}{\left(1 + \left|\frac{\gamma}{\gamma_r}\right|\right)} \qquad (4)$$

$$\gamma_r = \frac{\sigma'_m \sin\phi}{G} \qquad (5)$$

$$G = G_{ma}\left(\frac{\sigma'_m}{\sigma'_{ma}}\right)^{m_g} \qquad (6)$$

where G is the shear modulus (kN/m^2), τ is the shear stress (kN/m^2), γ is the shear strain, γ_r is the reference shear strain, σ'_m is the effective confining stress (kN/m^2), m_g is a parameter indicating the dependency on the confining pressure and $m_g = 0.5$ in based on [39]. The standard method for setting the parameters of the soil properties in [40] was followed in the present analysis. The effects of liquefaction were neglected.

TABLE I.   GROUND CONDITION

Soil	ρ (t/m^3)	G_{ma} (kN/m^2)	σ'_{ma} (kN/m^2)	ϕ (°)
Backfill sand	2.0	58300	89.8	38
Soil 1	2.0	72200	198.5	39
Soil 2	2.0	125000	279.2	39
Backfill stone	2.0	101250	98	40
Wall friction angle (°)	In front of the wall: $\delta = 15$ Behind the wall: $\delta = 0$			
Common physical properties	$h_{max} = 0.24$, $K_w = 2200000$ kN/m^2 $\nu = 0.33$			

ρ is the saturated unit weight, G_{ma} is the reference shear modulus, σ'_{ma} is the reference average effective confining stress, ϕ is the shear resistance angle, h_{max} is the maximum damping coefficient, K_w is the bulk modulus of pore water, ν is the Poisson's ratio.

TABLE II.   DIMENSIONS OF THE STRUCTURAL MEMBERS

Water depth (m)	Sheet pile		Tie rod	
	Depth of embedment (m)	Moment of inertia of area (m^4/m)	Area (m^2/m)	Length (m)
−5.5	−11.8	0.000104	0.00063	13.5
−11.0	−20.1	0.000791	0.00128	18.9

Water depth (m)	Anchor pile	
	Pile length (m)	Are moment of inertia (m^4/m)
−5.5	14.2	0.000304
−11.0	12.5	0.000516

Elastic modulus of all structural members is 200kN/mm^2

Sheet pile, anchor pile, and tie rod were modeled as linear beam elements. A thin steel-pipe pile was used as the anchor pile. Viscos boundaries were applied to both bottom and side boundaries. A bi-linear joint element was applied to the boundary between the wall (i.e. sheet pile and capping beam of the anchor pile) and the soil to consider wall friction. The friction between the tie rod and the soil was neglected. As the current study used 2D analysis, special care was required in setting the boundary conditions between the anchor pile and the surrounding soil. The 3D effect at the boundary between the soil and the pile was considered using a soil spring element [41]. The soil spring force k_{hp} calculated using (7) is proportional to the ratio of the increments of shear stress to shear strain of the soil ($d\tau/d\gamma$), where the coefficients α_p and β_p were selected according to the diameter and installation interval of the pile:

$$k_{hp} = \frac{\alpha_p d\tau}{\beta_p d\gamma} \qquad (7)$$

Figure 3 shows the FE mesh around the quay wall that was used in the calculations of water depth −5.5m as an example. The FE model had a horizontal length of 310m. The mesh height was set to transmit seismic waves up to 15Hz. Two ground motions were used in the calculations: the Hachinohe wave and the Iwakuni wave. These ground motions were calculated using seismic hazard analysis considering the source, path, and site amplification characteristics at the Hachinohe Port and Iwakuni Port, Japan, with a return period of 75 years [42]. The site amplification characteristics considered here are the ones due to shallow and deep subsurfaces [43–45]. Figure 4 shows the time history waveforms for the two ground motions. The maximum acceleration values were 1.0 and 1.5m/s^2 for the Hachinohe wave and the Iwakuni wave, respectively. The predominant frequency ranges are different between the Hachinohe and Iwakuni waves. The Hachinohe wave is dominated by low frequencies in the range of 0.4–1.5Hz, whereas the Iwakuni wave is dominated by high frequencies around 4.0Hz.

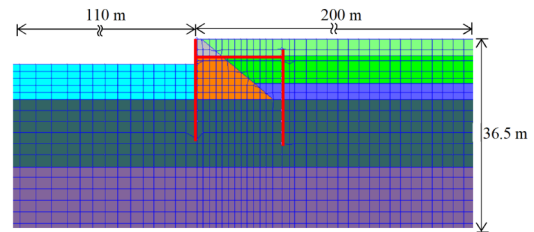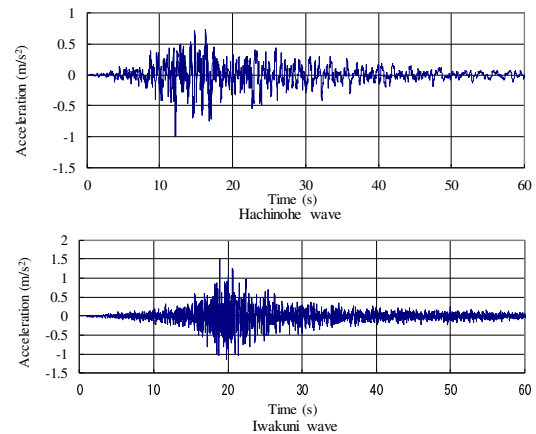
Fig. 3.   FE mesh.

Fig. 4.   Ground motion.

IV.   RESULTS AND DISCUSSION

A. *Effect of the Kinematic Force on the Deformation of Anchor Piles*

Figure 5 presents the residual displacement of the anchor pile calculated using FEA and the conventional method. The displacement of the anchor pile using the conventional method assumed the abovementioned nonlinear relationship between the pile displacement and subgrade reaction. The tie rod tensile force was set to the residual tensile force of the tie rod calculated by FEA, as shown in Table III.
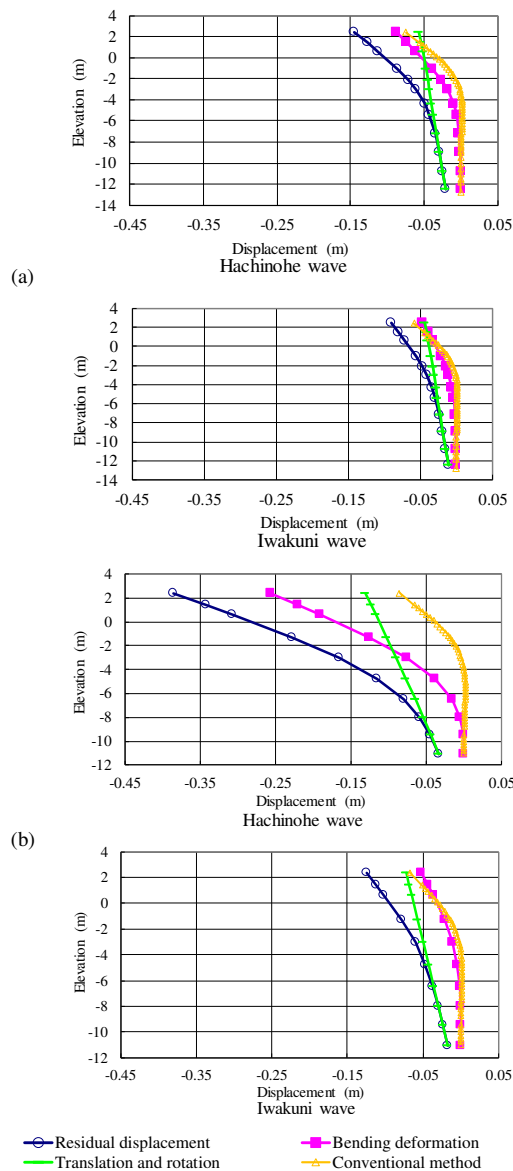
Fig. 5.   Displacement of an anchor pile. Water depth (a) -5.5m, (b) -11.0m.

TABLE III.   RESIDUAL TENSILE FORCE OF A TIE ROD

Water depth (m)	Hachinohe wave (kN)	Iwakuni wave (kN)
−5.5	216	185
−11.0	349	300

It is seen that the Hachinohe wave left larger displacements than the Iwakuni wave. The explanation is that the Hachinohe wave is dominated by the low frequency range, which has a large influence on ground deformation, while the Iwakuni wave is dominated by the high frequency range, which has a little influence on the ground deformation. The bending deformation was calculated using FEA by double integration of the residual curvature of the anchor pile when both the translation and rotation angles were zero at the pile tip. Translation and rotation were obtained by subtracting the bending deformation from the residual displacement. Translation and rotation at the

pile head were 30%–40% of the residual displacement, which cannot be neglected. The translational and rotational displacements are due to the kinematic force. No study has shown explicitly that the displacement of anchor pile includes three components, i.e. translation, rotation, and bending deformation, however, it can be confirmed by model experimental results [13] and analytical results [8] that the displacement of anchor pile includes components other than bending deformation.

In contrast, the conventional method assumes that the anchor pile is restrained by the ground at its base and cannot deform, so its deformation is only the bending deformation. The kinematic force is not considered in the conventional method, which contributes to its low estimation accuracy for the deformation degree of the anchor piles. Several studies estimated the amount of the anchor pile displacement assuming the occurrence of a slip line in the ground passing through the lower end of the anchor pile [15, 46]. However, it has been pointed out that the technique underestimates the displacement amount of the anchor pile [15]. To accurately calculate the displacement amount of the anchor pile, it is required to evaluate the kinematic force appropriately. When the degrees of bending deformation calculated by FEA and the conventional method are compared, the depth at which the bending deformation begins to increase greatly differs. Therefore, in the case of a Hachinohe wave applied to a quay wall with a water depth of −11m, the deformation at the pile head obtained by the conventional method is much smaller than that calculated by FEA. This difference is attributed to the differences in the resistive properties of the ground in front of the anchor pile assumed by the two methods.

B. Origins of the Kinematic Force

Sheet pile quay walls have a heterogeneous geometry, resulting in shear stresses being generated over a wide area of the nearby ground. Figure 6 shows a contour map of the initial shear stress. The initial shear stress above the seabed level is small in the active area behind the sheet pile and large in other areas between the sheet pile and the anchor pile. The initial shear stress below the seabed level is generated over a wide area around the sheet pile quay wall. For this reason, the shear stress of the ground fluctuates around the initial shear stress value, rather than zero, at the time of the earthquake. This leads to the generation of considerable shear strain during an earthquake due to the nonlinearity of the soil, which can result in significant residual ground deformation. To examine the influence of the initial shear stress on the residual deformation of the soil, 1D nonlinear seismic response analysis of the ground was performed by applying the initial shear stress extracted from the 2D FEA, where the initial shear stress refers to that at the positions shown in the red column in Figure 6. This is because the 1D analysis should use the initial shear stress free from the effects of the displacement of the anchor pile, and the large initial shear stress that causes soil deformation. As a reference, 1D analysis without the initial shear stress was also performed. Figure 7 compares the residual displacements of 1D analysis and 2D FEA results. In the case of the 2D FEA results, the translational and rotational displacements shown in Figure 5 are illustrated. As expected,

1D analysis without the initial shear stress resulted in almost no residual displacement, while 1D analysis with the initial shear stress resulted in a larger seaward residual displacement. Hence, the initial stress was found to act as implicit lateral force acting on the ground. The displacements determined by 1D analysis with the initial shear stress agreed well with those calculated by the 2D FEA.
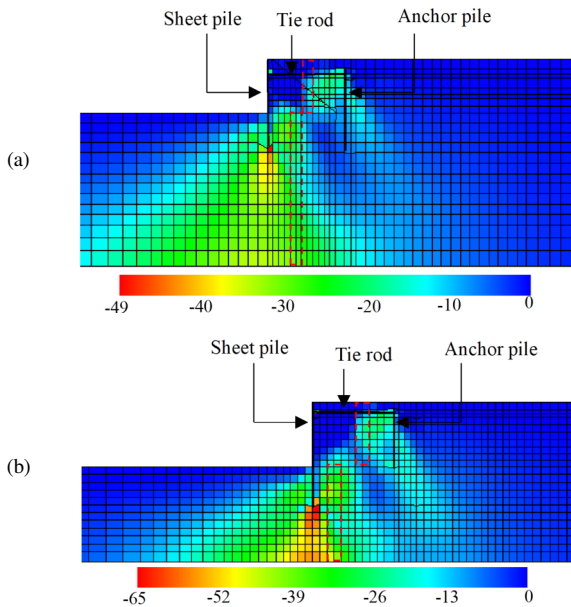

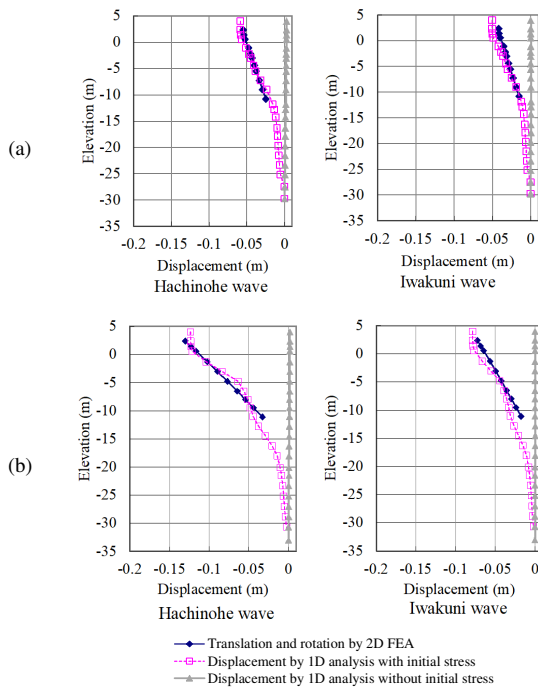Fig. 6. Contour map of the initial stress, water depth:(a) -5.5m, (b) -11m.

Fig. 7. Comparison of displacements. Water depth:(a) -5.5m, (b) -11m.

C. A Simplified Estimation Method of Anchor Pile Deformation under Kinematic Force

A simplified method for estimating the deformation of anchor piles under kinematic force is proposed in this paper, which does not require reference to the results of 2D FEA. Since a wharf constitutes irregular ground, the effective weight at the same depth is different in the ground at the front and the back of the sheet pile wall. Thus, shear stress is generated in the ground. An equation for calculating the ground shear stress when a distributed load is applied, based on Boussinesq's equation [47], is presented here. The simplified estimation method calculates the shear stress in the ground using the effective weight of the ground as a distributed load based on (8)-(10) and Figure 8.

$$\tau_{xy}(y) = \int_0^y \frac{\gamma_s}{2\pi} \cos 2\alpha_1(z)dz - \int_0^{y-H} \frac{\gamma_s}{2\pi} \cos 2\alpha_2 dz \quad (8)$$

$$\alpha_1(z) = -\tan^{-1}\frac{L_R}{y-z} \quad (9)$$

$$\alpha_2(z) = \tan^{-1}\frac{L_L}{y-H-z} \quad (10)$$

where γ_s is the unit weight of the ground (kN/m^3), z is the depth (m), α_1 and α_2 are the angles between the vertical line and the line connecting the estimation position and the edge of the distributed load (°), H is the wall height (m), L_R is the distance between the sheet pile wall and the anchor pile (m), and L_L is the distance from the sheet pile wall to the intersection of the passive failure line generated at the bottom of the sheet pile meets the seabed (m). The passive failure angle is 17° based on the Coulomb passive earth pressure.
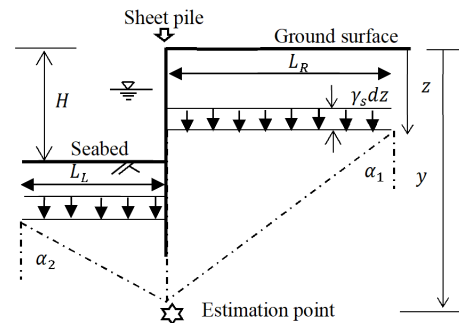

Fig. 8. Schematic diagram of the simplified estimation method for shear stress.

The first and second terms on the right side of (8) are the shear stress due to the effective weight of the ground behind and in front of the sheet pile wall, respectively. The range of the distributed load behind the sheet pile wall was determined from the wall to the anchor pile as the range where large shear stresses are generated (based on 2D FEA results). The range of the distributed load in front of the sheet pile wall is defined by the width of the passive failure region generated at the bottom of the sheet pile wall. This is assumed to be the region that mainly affects the shear stress. Since the simplified estimation method does not consider active failure regions behind the wall, the shear stress is maximum at the wall position, which was thus used to calculate the shear stress in the proposed estimation method.
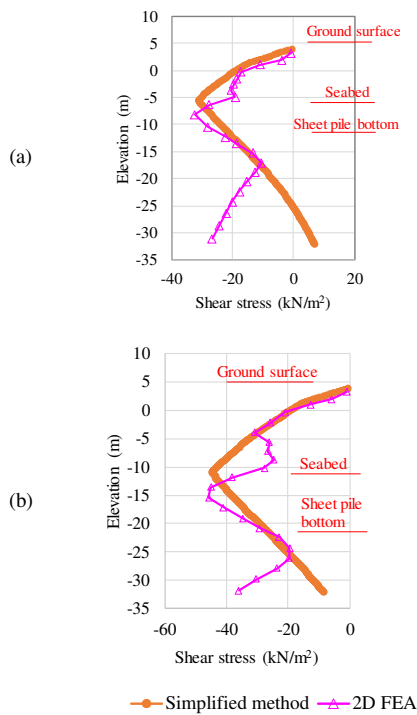
Fig. 9.   Comparison of the shear stress. Water depth:(a) -5.5m, (b) -11m.
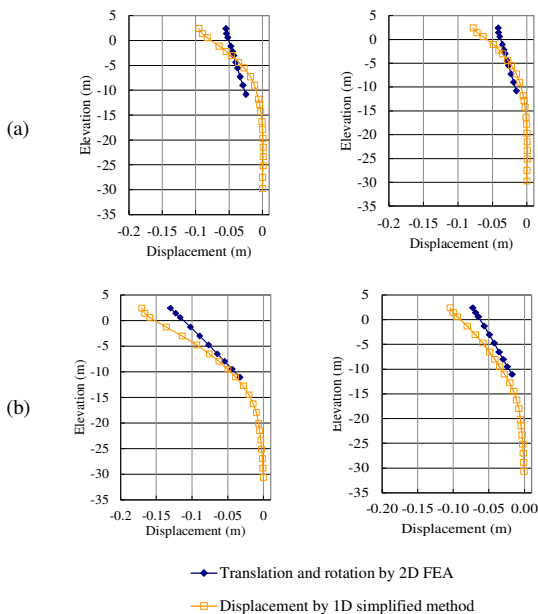

Fig. 10.   Comparison of the displacements under various conditions. Water depth:(a) -5.5m, (b) -11m. Left: Hachinohe wave, right: Iwakuni wave.

Figure 9 compares the shear stress estimated by the simplified method and that shown in Figure 6. Although the method somewhat overestimates the shear stress near the seabed, it generally reproduced the shear stress distribution obtained by the 2D FEA from the ground surface to the seabed. At depths below the seabed, the shear stress determined by 2D

FEA decreased from the seabed to a position slightly deeper than the sheet pile bottom and increased at deeper depths, whereas the shear stress determined by the simplified estimation method decreased monotonically below the seabed. However, it is assumed that the shear stress below the seabed has no significant effect on the degree of deformation of the anchor pile. The deformation obtained using the 1D simplified estimation method and the translational and rotational deformation of the anchor pile obtained by 2D FEA are compared in Figure 10. Although the deformation obtained by the simplified estimation method is a little larger than that obtained by the 2D FEA at the pile head, the results are in accordance in general. Therefore, the simplified estimation method is considered an effective method for estimating the degree of deformation of the anchor piles under kinematic forces.

V.   CONCLUSIONS

This study investigated the effect of kinematic forces on the deformation of the anchor pile of a sheet pile quay wall. The main conclusions drawn from the current study are:

- The deformation of the anchor pile due to the kinematic forces is 30%–40% of the total deformation at the pile head, which is a non-negligible amount. Therefore, the low accuracy of the deformation obtained by the conventional method is attributed to the fact that it only considers inertial and not kinematic forces.

- Shear stress is generated in the ground between the sheet pile and the anchor pile before an earthquake due to the irregular shape of the quay wall. This initial shear stress results in large shear deformation of the ground during an earthquake, resulting in kinematic forces acting on the anchor pile.

- A simplified method was proposed for estimating the shear stresses generated in the ground around the sheet pile quay wall and the deformation of the anchor pile under kinematic forces, without reference to the 2D FEA results. It was demonstrated that the simplified estimation method effectively reproduces the 2D FEA results, but with a much lower computational effort. Therefore, this strategy is useful for evaluating the deformation of anchor piles under kinematic force.

REFERENCES

[1]   *Technical standards and commentaries for port and harbour facilities in Japan*. Tokyo, Japan: The Overseas Coastal Area Development Institute of Japan, 2009.

[2]   *BS EN 1998-1(2004), Eurocode 8: Design of structures for earthquake resistance – Part 1: General rules, seismic actions and rules for buildings*. London, UK: British Standards Institution, 2004.

[3]   E. Galal, D. E. Mohamed, and E. Tolba, "A study of sheet pile quay wall rehabilitation methods," *Port-Said Engineering Research Journal*, vol. 26, no. 3, pp. 37–45, Sep. 2022, https://doi.org/10.21608/pserj.2022. 131369.1174.

[4]   G. A. Athanasopoulos *et al.*, "Lateral spreading of ports in the 2014 Cephalonia, Greece, earthquakes," *Soil Dynamics and Earthquake Engineering*, vol. 128, Jan. 2020, Art. no. 105874, https://doi.org/ 10.1016/j.soildyn.2019.105874.

[5]   S. Werner *et al.*, "Seismic Performance of Port de Port-au-Prince during the Haiti Earthquake and Post-Earthquake Restoration of Cargo

Throughput," *Earthquake Spectra*, vol. 27, no. 1, pp. 387–410, Oct. 2011, https://doi.org/10.1193/1.3638716.

[6] T. Sugano, A. Nozu, E. Kohama, K. Shimosako, and Y. Kikuchi, "Damage to coastal structures," *Soils and Foundations*, vol. 54, no. 4, pp. 883–901, Aug. 2014, https://doi.org/10.1016/j.sandf.2014.06.018.

[7] L. Wang, Z. Yajun, W. Gong, J. Li, and A. Ishimwe, "Calculation Method of Seismic Residual Displacement of Sheet Pile Quay Walls," *Advances in Civil Engineering*, vol. 2019, Aug. 2019, Art. no. e1251295, https://doi.org/10.1155/2019/1251295.

[8] G. Gazetas, E. Garini, and A. Zafeirakos, "Seismic analysis of tall anchored sheet-pile walls," *Soil Dynamics and Earthquake Engineering*, vol. 91, pp. 209–221, Dec. 2016, https://doi.org/10.1016/j.soildyn.2016.09.031.

[9] M. Mohajeri, Y. Kobayshi, K. Kawaguchi, and M. Sato, "Numerical Study on Lateral Spreading of Liquefied Ground Behind a Sheet Pile Model in a Large Scale Shake Table Test," in *13th World Conference on Earthquake Engineering*, Vancouver, BC, Canada, Aug. 2004, pp. 1–10.

[10] U. Cilingir, S. K. Haigh, S. P. G. Madabhushi, and X. Zeng, "Seismic behaviour of anchored quay walls with dry backfill," *Geomechanics and Geoengineering*, vol. 6, no. 3, pp. 227–235, Sep. 2011, https://doi.org/10.1080/17486025.2011.578670.

[11] A. Zekri, M. H. Aminfar, A. Ghalandarzadeh, and P. Ghasemi, "Effects of Liquefiable Layer for Dynamic Response of Anchored Flexible Quay Wall," in *10th International Congress on Advances in Civil Engineering*, Ankara, Turkey, Oct. 2012, pp. 1–10.

[12] K. Ichii, S. Iai, Y. Sato, and H. Liu, "Seismic Performance Evaluation Charts for Gravity Type Quay Walls," *Structural Engineering / Earthquake Engineering*, vol. 19, no. 1, pp. 21s–31s, 2002, https://doi.org/10.2208/jsceseee.19.21s.

[13] P. Ghasemi, A. Ghalandarzadeh, As. Zekri, and M. Aminfar, "Mitigation of Seismic Deformation of Anchored Quay Wall by Compacting," in *7th International Conference on Case Histories in Geotechnical Engineering*, Chicago, IL, USA, Dec. 2013, vol. 7th International Conference on Case Histories in Geotechnical Engineering, pp. 1–5.

[14] H. Tan, Z. Jiao, and J. Chen, "Field testing and numerical analysis on performance of anchored sheet pile quay wall with separate pile-supported platform," *Marine Structures*, vol. 58, pp. 382–398, Mar. 2018, https://doi.org/10.1016/j.marstruc.2017.12.006.

[15] C. J. W. Habets, D. J. Peters, J. G. de Gijt, A. Metrikine, and S. N. Jonkman, "Model Solutions for Performance-Based Seismic Analysis of an Anchored Sheet Pile Quay Wall," *International Journal of Civil, Environmental, Structural, Construction and Architectural Engineering*, vol. 10, no. 3, pp. 248–260, 2016.

[16] M. F. R. Khazi and M. Vazeer, "FEM analysis of anchored sheet pile quay wall: A case study on the failure of WQ-7 berth of Visakhapatnam port," *International Journal of Research in Engineering and Technology*, vol. 5, no. 14, pp. 25–31, Sep. 2016, https://doi.org/10.15623/ijret.2016.0526006.

[17] Y.-Y. Ko and H.-H. Yang, "Deriving seismic fragility curves for sheet-pile wharves using finite element analysis," *Soil Dynamics and Earthquake Engineering*, vol. 123, pp. 265–277, Aug. 2019, https://doi.org/10.1016/j.soildyn.2019.05.014.

[18] T. Hamamoto, T. Nagano, and T. Yamao, "Analytical study of the sheet pile quay damaged by 2005 Fukuoka earthquake," in *Proceedings of 8th Annual IIIRR Conference on Disaster Management*, Kumamoto, Japan, 2012, pp. 134–141.

[19] K. Tokimatsu and Y. Asaka, "Effects of Liquefaction-Induced Ground Displacements on Pile Performance in the 1995 Hyogoken-Nambu Earthquake," *Soils and Foundations*, vol. 38, pp. 163–177, Sep. 1998, https://doi.org/10.3208/sandf.38.Special_163.

[20] S. Nikolaou, G. Mylonakis, G. Gazetas, and T. Tazoh, "Kinematic pile bending during earthquakes: analysis and field measurements," *Geotechnique*, vol. 51, no. 5, pp. 425–440, Jun. 2001, https://doi.org/10.1680/geot.2001.51.5.425.

[21] M. N. Hussien, T. Tobita, S. Iai, and M. Karray, "Soil-pile-structure kinematic and inertial interaction observed in geotechnical centrifuge experiments," *Soil Dynamics and Earthquake Engineering*, vol. 89, pp. 75–84, Oct. 2016, https://doi.org/10.1016/j.soildyn.2016.08.002.

[22] K. Tokimatsu, H. Suzuki, and M. Sato, "Effects of inertial and kinematic interaction on seismic behavior of pile with embedded foundation," *Soil Dynamics and Earthquake Engineering*, vol. 25, no. 7, pp. 753–762, Aug. 2005, https://doi.org/10.1016/j.soildyn.2004.11.018.

[23] R. W. Boulanger, C. J. Curras, B. L. Kutter, D. W. Wilson, and A. Abghari, "Seismic Soil-Pile-Structure Interaction Experiments and Analyses," *Journal of Geotechnical and Geoenvironmental Engineering*, vol. 125, no. 9, pp. 750–759, Sep. 1999, https://doi.org/10.1061/(asce)1090-0241(1999)125:9(750).

[24] J.-S. Chiou, W.-Y. Hung, Y.-T. Lee, and Z.-H. Young, "Combined dynamic structure-pile-soil interaction analysis considering inertial and kinematic effects," *Computers and Geotechnics*, vol. 125, Sep. 2020, Art. no. 103671, https://doi.org/10.1016/j.compgeo.2020.103671.

[25] N. Mononobe, "On determination of earth pressure during earthquake," in *World Engineering Congress*, Tokyo, Japan, 1929, vol. 9, pp. 177–185.

[26] H. Matlock, "Correlation for Design of Laterally Loaded Piles in Soft Clay," in *2nd Annual Offshore Technology Conference*, Houston, TX, USA, Apr. 1970, https://doi.org/10.4043/1204-MS.

[27] M. Georgiadis, C. Anagnostopoulos, and S. Saflekou, "Cyclic Lateral Loading of Piles in Soft Clay," *Journal of Geotechnical Engineering*, vol. 23, no. 1, pp. 47–60, Jun. 1992.

[28] M. D. Dewaikar and S. D. Patil, "Behavior of Laterally Loaded Piles in Cohesionless Soil under One-Way Cyclic Loading," in *The New Millennium Conference*, 2001, pp. 97-100.

[29] T. Nagao, "Effect of Foundation Width on Subgrade Reaction Modulus," *Engineering, Technology & Applied Science Research*, vol. 10, no. 5, pp. 6253–6258, Oct. 2020, https://doi.org/10.48084/etasr.3668.

[30] T. Nagao and R. Tsutaba, "Evaluation Methods of Vertical Subgrade Reaction Modulus and Rotational Resistance Moment for Seismic Design of Embedded Foundations," *Engineering, Technology & Applied Science Research*, vol. 11, no. 4, pp. 7386–7392, Aug. 2021, https://doi.org/10.48084/etasr.4269.

[31] S. Iai, Y. Matsunaga, and T. Kameoka, "Strain Space Plasticity Model for Cyclic Mobility," *Soils and Foundations*, vol. 32, no. 2, pp. 1–15, Jun. 1992, https://doi.org/10.3208/sandf1972.32.2_1.

[32] S. Iai and T. Kameoka, "Finite Element Analysis of Earthquake Induced Damage to Anchored Sheet Pile Quay Walls," *Soils and Foundations*, vol. 33, no. 1, pp. 71–91, Mar. 1993, https://doi.org/10.3208/sandf1972.33.71.

[33] S. Higuchi *et al.*, "Evaluation of the seismic performance of dual anchored sheet pile wall," in *15th World Conference on Earthquake Engineering*, Lisbon, Portuga, Sep. 2012, pp. 1–10.

[34] T. Nagao and Y. Kurachi, "An Experimental and Analytical Study on the Seismic Performance of Piers with Different Foundation Bottom Widths," *Engineering, Technology & Applied Science Research*, vol. 12, no. 5, pp. 9142–9148, Oct. 2022, https://doi.org/10.48084/etasr.5088.

[35] I. Towhata and K. Ishihara, "Modelling soil behavior under principal stress axes rotation," in *International Conference on Numerical Methods in Geomechanics*, Nagoya, Japan, 1985, pp. 523–530.

[36] B. O. Hardin and V. P. Drnevich, "Shear Modulus and Damping in Soils: Design Equations and Curves," *Journal of the Soil Mechanics and Foundations Division*, vol. 98, no. 7, pp. 667–692, Jul. 1972, https://doi.org/10.1061/JSFEAQ.0001760.

[37] G. Masing, "Eigenspannugen und Verfestigung beim Messing," in *Second International Congress of Applied Mechanics*, Zurich, Switzerland, 1926, pp. 332–335.

[38] O. Ozutsumi and S. Iai, "Adjustment Method of the Hysteresis Damping for Multiple Shear Spring Model," in *4th International Conference on Recent Advances in Geotechnical Earthquake Engineering and Soil Dynamics*, San Diego, CA, USA, Mar. 2001.

[39] I. Suetomi and N. Yoshida, "Nonlinear Behavior of Surface Deposit during the 1995 Hyogoken-Nambu Earthquake," *Soils and Foundations*, vol. 38, pp. 11–22, Sep. 1998, https://doi.org/10.3208/sandf.38.Special_11.

[40] T. Morita, "Simplified method to determine parameter of FLIP," *Technical note of the Port and Harbour Research Institute*, vol. 869, pp. 1–36, 1997.

[41] O. Ozutsumi, Y. Tamari, Y. Oka, K. Ichii, S. Iai, and Y. Umeki, "Modeling of soil-pile interaction subjected to soil liquefaction in plane strain analysis," in *53rd Japan National Conference on Geotechnical Engineering*, Takamatsu, Japan, 2003, pp. 1899-1900.

[42] T. Nagao, M. Yamada, and A. Nozu, "Probabilistic Seismic Hazard Analysis with Focus on Fourier Amplitude and Group Delay Time," in *15th World Conference on Earthquake Engineering*, Lisbon, Portuga, Sep. 2012, pp. 1–10.

[43] T. Nagao, "Seismic Amplification by Deep Subsurface and Proposal of a New Proxy," *Engineering, Technology & Applied Science Research*, vol. 10, no. 1, pp. 5157–5163, Feb. 2020, https://doi.org/10.48084/etasr.3276.

[44] T. Nagao and Y. Fukushima, "Source- and Site-Specific Earthquake Ground Motions: Application of a State-of-the-Art Evaluation Method," *Engineering, Technology & Applied Science Research*, vol. 10, no. 4, pp. 5882–5888, Aug. 2020, https://doi.org/10.48084/etasr.3612.

[45] T. Nagao, "Maximum Credible Earthquake Ground Motions with Focus on Site Amplification due to Deep Subsurface," *Engineering, Technology & Applied Science Research*, vol. 11, no. 2, pp. 6873–6881, Apr. 2021, https://doi.org/10.48084/etasr.3991.

[46] C.-Y. Ku, J.-J. Jang, J.-Y. Lai, and M.-J. Hsieh, "Modeling of dynamic behavior for port structures using the performance-based seismic design," *Journal of Marine Science and Technology*, vol. 25, no. 6, pp. 732–741, Dec. 2017, https://doi.org/10.6119/JMST-017-1226-14.

[47] J. H. Michell, "On the Direct Determination of Stress in an Elastic Solid, with application to the Theory of Plates," *Proceedings of the London Mathematical Society*, vol. s1-31, no. 1, pp. 100–124, 1899, https://doi.org/10.1112/plms/s1-31.1.100.